

Efficient Bayesian Inference of Miter Gates using High-Fidelity Models

Manuel A. Vega, Mukesh K. Ramancha, Joel P. Conte, Michael D. Todd

Department of Structural Engineering
Jacobs School of Engineering
University of California San Diego, La Jolla, CA 92093

Abstract Continuous monitoring of miter gates used in navigation locks is desirable in order to prioritize maintenance and avoid unexpected failures. Substantial economic losses to the marine cargo and associated industries are caused by the closure of these inland waterway structures. Strain gauges are often installed in many of these miter gates for data collection, and various inverse finite element techniques are used to convert the strain gauges data to damage-sensitive features. One of the damage features is the development of a contact-loss “gap” between the components (i.e. quoin blocks) that support the gate laterally, which leads to load re-distribution that can induce overload in some components of the gate. Arguably, a refined finite element model of such structure can be very computationally expensive even when using linear models. An efficient way to solve an inverse problem with time-consuming model evaluations is making use of parallel model evaluations using a Sequential Monte Carlo (SMC) algorithm and parallel solution of the finite element (FE) equations using a commercial FE software. A significant advantage of SMC algorithms is that model evaluations are independent and are able to be run in parallel. In this paper, an expensive high fidelity model of a miter gate is used to infer the gap extend given a noisy set of strain measurements.

Keywords: Miter Gates, Finite Element Model Updating, Inverse Problem, Model Bias , Batch Bayesian Inference, Sequential Monte Carlo.

1. Introduction

Navigation locks form a crucial part of inland waterways infrastructure network. Miter gates are the most common type of navigation locks in the United States (US) with other types of lock gates being sector, tainter, and vertical lift [1]. Miter gates are steel structures that allow passage of ships, boats, and watercrafts across stretches of different water levels in canals and rivers. In the US, more than half of these structural assets have surpassed their 50-year economic design life [2]. Damage to miter gates may lead to closure of a lock chamber. Two types of maintenance events (i.e., scheduled and unscheduled) apply to miter gates. Scheduled maintenance allows navigation users to adjust their activities to avoid unexpected delays and minimize their economic loss. However, unscheduled closures resulting from unexpected events such as undetected deterioration reaching a critical limit state or extreme events (e.g., barge impact) more substantially affect navigation users’ economic bottom line and induce a higher cost of maintenance [3]. Estimating the condition of a miter gate and its components can help to reduce the risk in unscheduled maintenance events and prioritizing better schedule maintenance events. The U.S. Army Corps of Engineers (USACE) have established a discrete rating system to allow inspectors to rate the components of a miter gate based on condition and performance [4], which are used by decision-makers for maintenance and operations planning. However, inspections based on this rating system can vary for different inspectors because it is based on engineer judgement. Continuous structural health monitoring (SHM) of these infrastructure assets may help to reduce the uncertainty and ensure better-informed decisions that lead to safer and more reliable operations [5].

One of the consequences of deterioration in miter gates is the formation of a bearing gap that occurs between the contact blocks that interface the lock walls and the miter gate [6]. The bearing gap governs the lateral boundary conditions on the gate, and its degradation from loading, wear, corrosion, and other sources leads to changes in the stress-strain profile of the entire miter gate [7]. Experienced inspectors and lock operators have indicated the importance of knowing the condition of contact block and its role in identifying load transfer issues in the gate [2], [8]. Other analyses would have to be conducted to determine the critical gap parameters (size, location, etc.) that lead to some failure in the gate or in one of its components. Alternatively, the boundary conditions may also be obtained by inferring directly the forces that support the gate laterally [9].

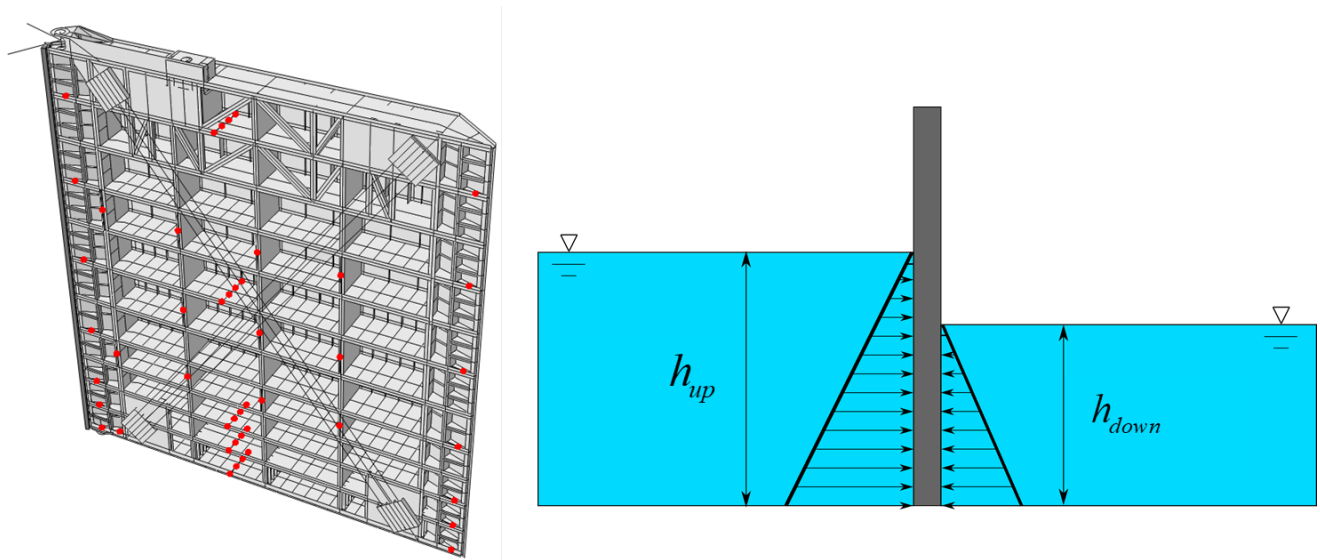
Many of the miter gates owned by USACE are instrumented with strain gauges for data acquisition [10]. The relationship between the formation of the bearing gap and the stress-strain profile in the entire gate can be better understood by using a finite element (FE) model. For a SHM system, the inverse relation between the input and outputs of the FE model are desired. This inverse relation can be estimated by performing Bayesian inference that uses FE model evaluations. A Bayesian approach is desirable because it is able to quantify the risk on making decisions such as corrective maintenance of components. Many

56 powerful algorithms that perform Bayesian inference can be used to solve this problem [11]. However, many of these
57 algorithms are not feasible for real-time health monitoring.

58
59 In this paper, a Bayesian Inversion of High Fidelity FE model is accomplished by using the sequential Monte Carlo (SMC)
60 algorithm to perform Bayesian inference. This algorithm was selected due to the accuracy in its predictive capabilities and its
61 parallelizable capabilities to perform (FE) model evaluations [12]. The paper first explains the finite element model and then
62 describes two modelling options for the bearing gap. In the next section, Bayesian inference on miter gates are explained and
63 results are shown for two different levels of complexity. The results show the effect of aleatory and epistemic uncertainties
64 considered in this miter gate problem. Finally, a conclusion and further work section discusses the additional steps to be taken
65 before deploying a SHM system in miter gates and the issues of dealing with model uncertainty.

66 67 2. Testbed Structure and Finite Element Modeling

68
69 In this research, the Greenup miter gate/lock located on the Ohio river is used as the testbed structure. A physics-based FE
70 model of the gate was developed in ABAQUS software, shown in Figure 1a. This FE model has been validated using the
71 measured strain gauge readings [2]. The Greenup gate is a brand-new gate where a negligible gap (“undamaged” condition)
72 was assumed for validation purposes. 3D linear shells elements were used to reduce the computational cost of such a large
73 model. Figure 1b shows the side view of a miter gate that is subjected to upstream and downstream hydrostatic forces.
74



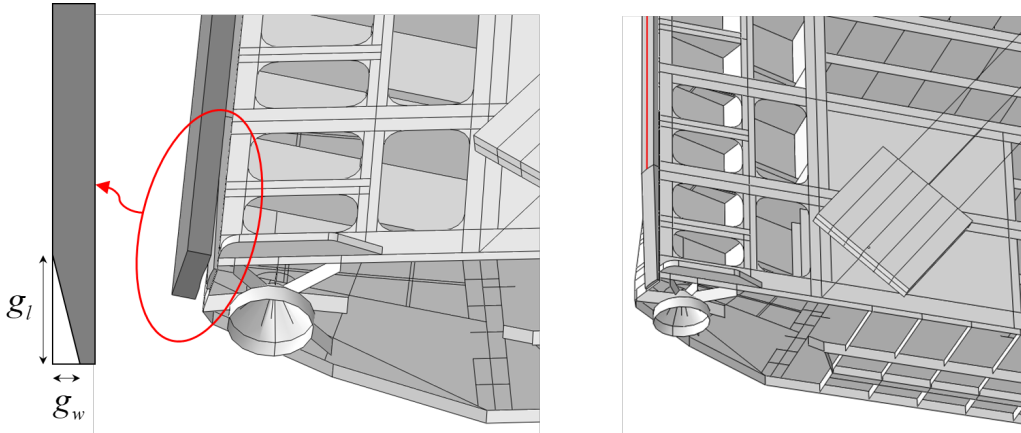
75
76 Figure 1: FE model of Greenup Gate with sensor locations and loading conditions

77 78 2.1 Modelling Options for Gap Formation

79
80 The gap formation between the contact (quoin) blocks control how the gate is supported laterally and consequently introduces
81 a change in the stress/strain distribution of the entire gate, especially in the pintle area where the gate is supported by a pintle
82 ball. For modelling purposes, the pintle ball where the gate rest is idealized as a pin support. In this paper damage is introduced
83 by controlling the extent of the gap. In order to model the gap itself, two different modelling approaches are presented in this
84 work:

85
86 *Option 1:* A contact-type constraint is used between the contact blocks as shown in Figure 2a, making this a computationally
87 expensive nonlinear problem. To impose the contact constraint, the Lagrange multiplier method was employed. The strain
88 gauge locations are far from the contact area, mostly due to physical constraints in the miter gate, but this far-field location also
89 mitigates errors due to the method employed to enforce the contact constraint. The opposite side of the wall quoin block uses
90 fixed boundary conditions, and symmetry boundary conditions are used at the right end (i.e., miter) of the gate to simulate the
91 right leaf. The variables g_l and g_w denote the gap length and depth, respectively.

92



93
94 Figure 2: a) Option 1: Using contact between wall quoin block and gate quoin block, and b) Option 2: Pin boundary
95 conditions along the gate quoin block (restrained in x and y directions) except at gap location

96 *Option 2:* Pin boundary conditions are used directly to support the gate quoin block instead of modelling the wall quoin block
97 and using a contact algorithm to support the gate laterally. To model the effect of the gap formation a particular length (g_l) of
98 the gate quoin block is left unrestrained as shown in Figure 2b. This representation may not be as accurate as Option 1, but it
99 is a more attractive option computationally, since it is a linear FE model.

100
101 The main difference in the physics between Option 1 and 2 is that Option 1 captures the effect of partial gap closure after the
102 gate is subjected to hydrostatic loads. However, since the portion of the gap that closes is small under most loading scenarios,
103 Option 2 is a reasonable alternative choice.

104 105 3. Estimating Gap Length in Miter Gates using Bayesian Inference

106
107 For given hydrostatic inputs and gap parameters, the FE model could be evaluated as a “forward model” to yield the resulting
108 strain field resulting in the gate; consequently, solving an inverse problem is necessary to obtain the gap length value, g_l , given
109 a set of strain measurements obtained at different locations on the miter gate. There are two general ways often used to solve
110 an inverse problem: 1) a Bayesian approach, which computes a posterior distribution of the model parameters given prior
111 knowledge and the data, or 2) a regularized data fitting approach, which chooses an optimal model [13] by minimizing an
112 objective function that minimize the empirical risk (i.e. training error). In SHM, estimates of gap length (or other damage
113 parameters) are meaningful to the decision-making process of operators and stakeholders. Therefore, the Bayesian approach is
114 desired to obtain estimates of the gap length that can help to understand the current damage state of a miter gate. In the Bayesian
115 approach, the posterior distribution of the model parameters (e.g. gap length) can be obtained from:

$$116$$

$$117 \quad p(g_l, \sigma_{strain} | y) \propto p(y | g_l, \sigma_{strain}) p(g_l, \sigma_{strain}),$$

118
119 where

$$120 \quad \underset{\text{measured response}}{\mathbf{y}} = \underset{\text{FE predicted response}}{\mathbf{h}(g_l, \mathbf{u})} + \underset{\text{error/noise}}{\mathbf{w}},$$

121
122 and where \mathbf{y} represents the strain measurement at gages location, \mathbf{u} represents the hydrostatic loading conditions (i.e. h_{up} and
123 h_{down}), and \mathbf{w} is assumed to be a zero-mean uncorrelated gaussian distribution as follows:

$$124$$

$$125 \quad \mathbf{w} \sim N \left(\underset{46 \times 1}{\mathbf{0}}, \underset{46 \times 46}{\sigma_{strain}^2 \mathbf{I}} \right)$$

$$126 \quad \boldsymbol{\theta} = [g_l, \sigma_{strain}]^T \in \sim^2.$$

127
128 The posterior distribution of the parameters is typically mathematically intractable due to the normalization term (see Eq. (1)).
129 In this work, the computation of the posterior is accomplished by using the SMC algorithm to perform Bayesian inference.

130 This algorithm was selected due to the accuracy in its predictive capabilities and its parallelizable capabilities to perform (FE)
 131 model evaluations.

132

133 3.1 Batch Inference using SMC

134

135 Sequential Monte Carlo (SMC) or Transitional Markov chain Monte Carlo (TMCMC) methods are a class of simulation-based
 136 Bayesian inference techniques which sample from the complete joint posterior distribution of the unknown parameter vector
 137 $\boldsymbol{\theta}$. SMC methods do not impose any assumptions on the probability structure prior and the posterior; hence, these methods are
 138 applicable in very general settings. SMC methods are inherently parallelizable, therefore ideal for solving the inverse problem
 139 involving computationally-expensive FE model evaluations.

140

141 The idea of SMC is to avoid directly sampling the target PDF (posterior) but rather sample an easier-to-sample PDF and then
 142 weigh, resample, and perturb the samples to describe the target PDF. To achieve this, SMC constructs a series of intermediate
 143 PDFs, known as tempered posteriors, that start from prior distribution (easy to sample) and converge to the posterior distribution
 144 (hard to sample) as follows

145

$$146 \underbrace{p(\boldsymbol{\theta} | D)_j}_{\text{tempered posterior}} \propto p(D | \boldsymbol{\theta})^{\beta_j} \times \underbrace{p(\boldsymbol{\theta})}_{\text{prior}} \quad j = 0, 1, \dots, m \quad 0 = \beta_0 < \beta_1 < \dots < \beta_m = 1,$$

147

148 where β_j is the tempering parameter at stage j . When $\beta_j = 0$ at the initial stage ($j = 0$), the tempered posterior $p(\boldsymbol{\theta} | D)_0$
 149 is just the prior $p(\boldsymbol{\theta})$, and when $\beta_j = 1$ at the final stage ($j = m$) the tempered posterior $p(\boldsymbol{\theta} | D)_m$ is the target posterior
 150 $p(\boldsymbol{\theta} | D)$. SMC represents the tempered posterior distribution at every stage by a set of weighted samples (also called particles).
 151 SMC approximates j^{th} stage tempered posterior $p(\boldsymbol{\theta} | D)_j$ by weighing, resampling, and perturbing (using Markov chain
 152 Monte Carlo) the particles of $j-1^{\text{th}}$ stage tempered posterior $p(\boldsymbol{\theta} | D)_{j-1}$. The SMC algorithm for sampling the target posterior
 153 is shown in Table 1.
 154

Table 1: SMC Algorithm

<p>Let N be the number of particle (or weighted samples) at every stage, and ESS_j be the effective sample size at stage j</p> <p>Initialize N, $j = 0$, $ESS_0 = N_p$, $\beta_0 = 0$</p> <p>Generate N samples $\{\boldsymbol{\theta}_{j=0}^i; i = 1, \dots, N\}$ from the prior distribution $p(\boldsymbol{\theta})$</p> <p>while tempering parameter $\beta_j < 1$</p> <ul style="list-style-type: none"> • increase stage number $j = j + 1$ • choose $\tilde{\beta}_j$ such that $ESS_j = 0.95 \times ESS_{j-1}$, $\beta_j = \min(\tilde{\beta}_j, 1)$ • <u>weighting</u>: $w_j^i = p(D \boldsymbol{\theta}_{j-1}^i)^{\beta_j - \beta_{j-1}}$ for $i = 1, \dots, N$ • <u>resampling</u>: $\tilde{\boldsymbol{\theta}}_j^i = \boldsymbol{\theta}_{j-1}^i$ with probability w_j^i for $i = 1, \dots, N$ • <u>perturbation</u>: start an MCMC chain at $\tilde{\boldsymbol{\theta}}_j^i$ and take N_{MCMC} steps with target distribution $p(\boldsymbol{\theta} D)_j$ for each $i = 1, \dots, N$. Gather last sample of each MCMC chain to obtain $\{\boldsymbol{\theta}_j^i; i = 1, \dots, N\}$ <p>end</p> <p>$\{\boldsymbol{\theta}_j^i; i = 1, \dots, N\}$ are the samples of the target posterior $p(\boldsymbol{\theta} D)$</p>

155

156 4. Three-stage approach

157

158 Implementing a real SHM monitoring system will, arguably, involve several types of uncertainties that will affect the estimation
 159 process shown previously. One of the main sources of discrepancy between the estimation and the true model parameter values
 160 is due to model uncertainties, i.e., how the forward model (e.g. FE model) used in the inference process differs from the true
 161 physical model. To systematically tackle this problem, a 3-stage approach is used to start accounting for model uncertainties
 162 as shown in Figure 3.
 163

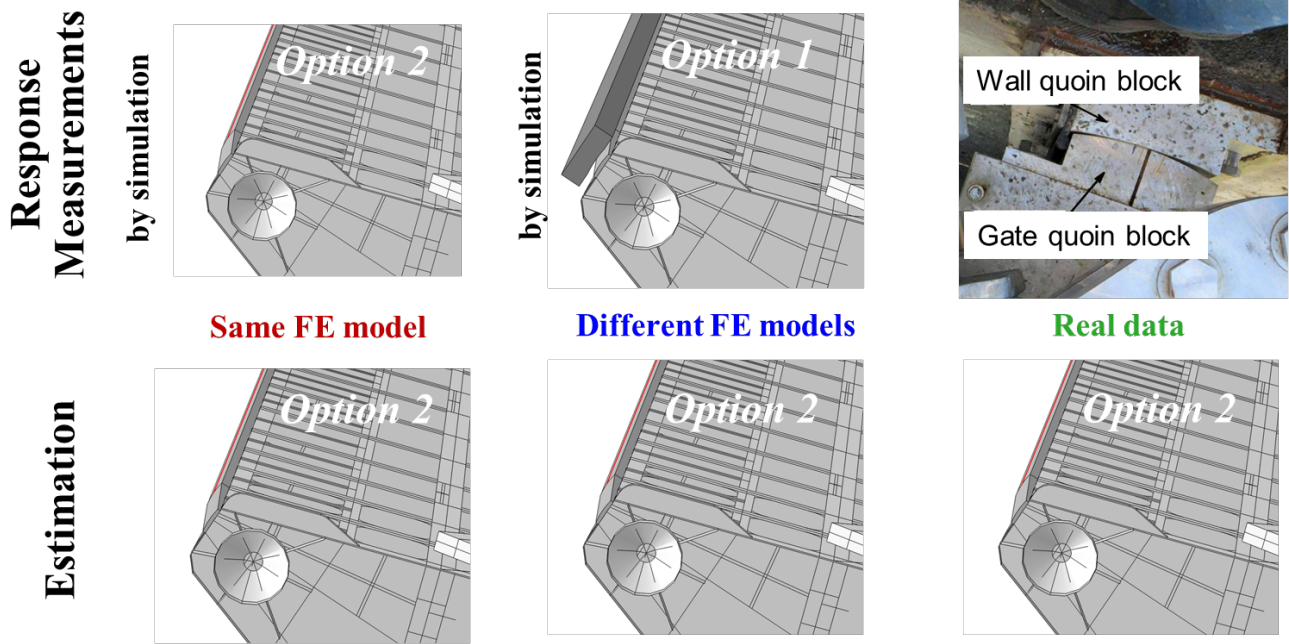


Figure 3: Systematic and progressive approach to handle various sources of uncertainties.

4.1 Stage 1: Same FE model

As shown in Figure 3, stage 1 uses the same FE models to represent the physical model used for estimation and the true physical model used to obtain the response measurements. Clearly, model uncertainty is not considered in this stage. As described earlier, there are two competing gap models. Option 2 is used as the FE model in this case due to its fast model evaluations. The estimation of the gap length for a specific response measurement is shown in Figure 4. The parameter δ is the estimated coefficient of variation, and r is the Pearson correlation coefficient.

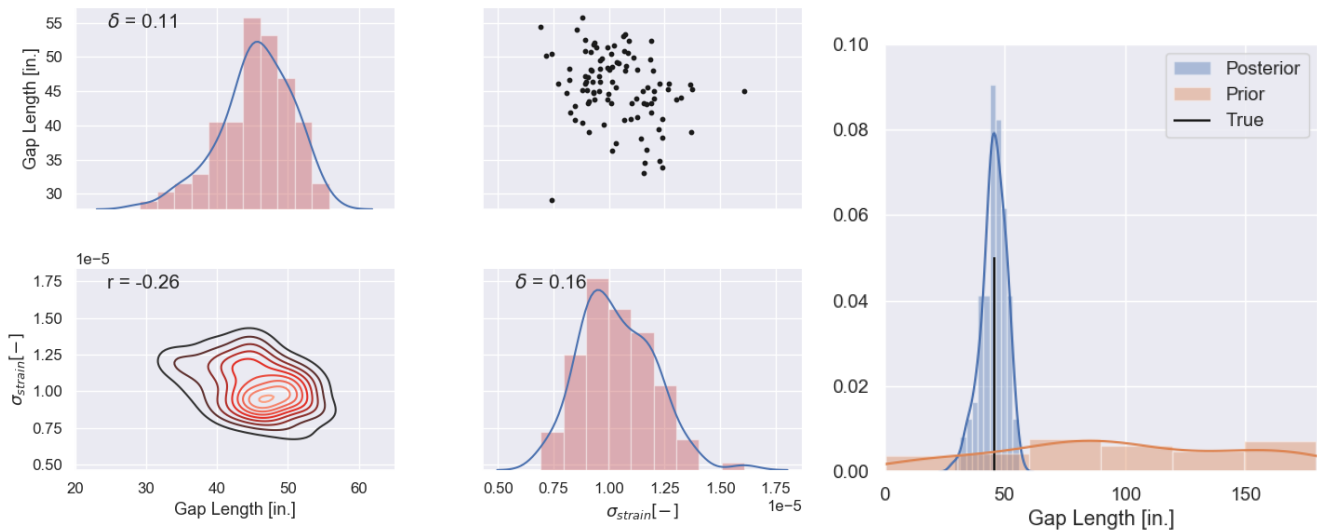
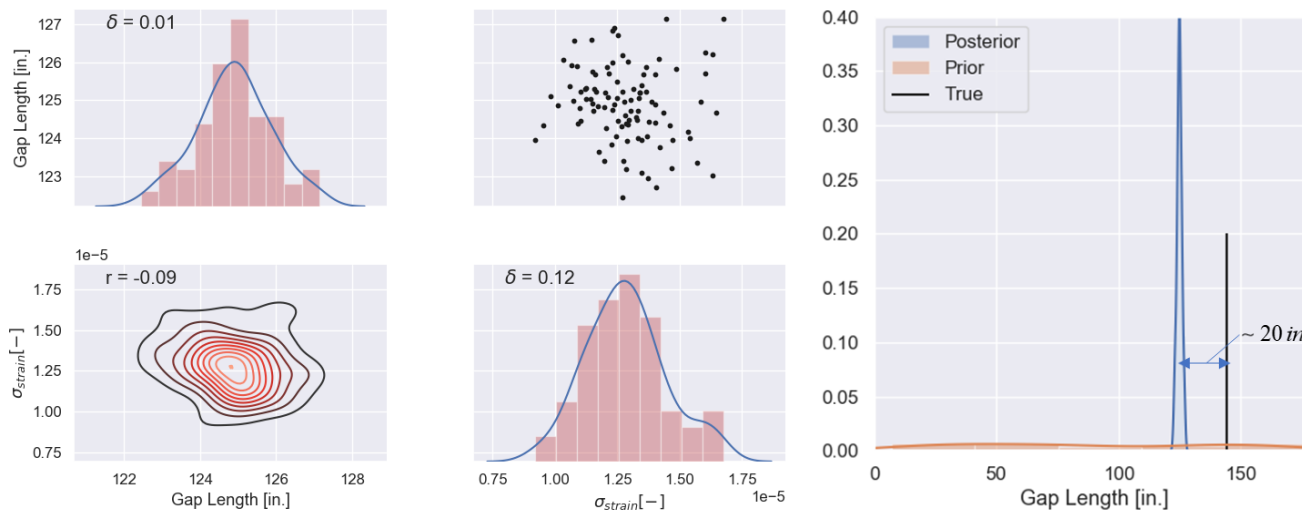


Figure 4: a) Joint posterior distribution using 100 particles, and b) prior and posterior distributions vs true value

179 As intended the posterior distribution covers the true value of the gap length and also the standard deviation of the (noise) error.
 180 The gap length prior distribution used for the inference follows a uniform distribution between 0 in and 180 in. These values
 181 are based on inputs from experienced lock operators.
 182

183 4.2 Stage 2: different FE models

184
 185 As shown in Figure 3, stage 2 uses different FE models to represent the physical model used for estimation (option 2) and the
 186 true physical model (option 1) used to obtain simulated response measurements. Model uncertainty is considered in this case,
 187 as the way that the gap between contacts blocks is modelled is very different between options 1 and 2. The gap depth is assumed
 188 to be 0.25 in for modelling option 1, which is used to simulate the true physical process and obtain the measurement response.
 189



190
 191 Figure 5: a) Joint posterior distributions using 100 particles, and b) prior and posterior distributions vs true value
 192

193 The posterior distribution of the gap length is very confident at a gap length around 124 in, while the true simulated gap length
 194 is equal to 144 in. Therefore, for this singular case the posterior estimation is biased by ~20 in. These results are very consistent
 195 with the values obtained by Brynjarsdottir and O'Hagan [14] when two different models are used to represent the physical
 196 model used for estimation and true physical model used to obtain simulated response measurements
 197

198 4.3 Stage 3: Real data

199
 200 As shown in Figure 3, stage 3 uses real SHM data for the response measurements and a FE model to simulate the physical
 201 model used for estimation. For this step, a fully FE model should be validated at different damage levels, which in practice it
 202 is challenging to obtain. Also, additional parameters (e.g. critical crack, corrosion, uncertainty in the material, amount of
 203 prestress in the diagonals, etc.) that are strain-sensitive should be identified to improve the predictive capabilities of this
 204 problem.
 205

206 5. Conclusions and Further Work

207
 208 A miter gate gap estimation is accomplished by perform Bayesian inference using a validated high-fidelity FE model. Two
 209 different models are presented to simulate damage (formation of gap), and a comparison of their predictive capabilities is
 210 performed using a Bayesian approach. The use of the SMC algorithm in large FE models is encouraging due to its parallelizable
 211 capabilities. Often, a (surrogate) data-driven model is created to replace an expensive FE model, but this was not needed in this
 212 work. Physics-based models may be a better option for extrapolation, however, especially when limited damage data is
 213 available. Additional steps need to be taken before deploying a SHM system in miter gates specially when dealing with model
 214 uncertainty. To further improve the predictive capabilities of cases in stage 2 and 3, a bias function can be trained to learn the
 215 model uncertainty between two models as described in detail in [14]–[17]. Again, this bias function should be carefully
 216 studied/interpreted when using them for interpolation or extrapolation. Additionally, a sensitivity analysis should be studied to
 217 understand the sensitivity of the strain gages to different model parameters, as this may also lead to improved predictive
 218 capabilities.

219
220
221
222
223
224
225
226
227
228
229
230
231
232
233
234
235
236
237
238
239
240
241
242
243
244
245
246
247
248
249
250
251
252
253
254
255
256
257
258
259
260
261
262
263
264
265

6. Acknowledgements

Funding for this work was provided by the United States Army Corps of Engineers through the U.S. Army Engineer Research and Development Center Research Cooperative Agreement W912HZ-17-2-0024.

7. References

- [1] Q. Alexander, A. Netchaev, M. Smith, C. Thurmer, and J. D. Klein, “Telemetry techniques for continuous monitoring of partially submerged large civil infrastructure,” in *Sensors and Smart Structures Technologies for Civil, Mechanical, and Aerospace Systems 2018*, 2018, vol. 1059823, no. March, p. 76.
- [2] S. D. Foltz, “Investigation of Mechanical Breakdowns Leading to Lock Closures,” Champaign, IL, 2017.
- [3] M. M. Kress *et al.*, “ERDC / CHL TR-16-8 Marine Transportation System Performance Measures Research Coastal and Hydraulics Laboratory,” Vicksburg, MS, 2016.
- [4] M. A. Vega, R. Madarshahian, T. B. Fillmore, and M. D. Todd, “Optimal Maintenance Decision for Deteriorating Components in Miter Gates using Markov Chain Prediction Model,” in *12th International Workshop on Structural Health Monitoring*, 2019.
- [5] B. A. Eick *et al.*, “Automated damage detection in miter gates of navigation locks,” *Struct. Control Heal. Monit.*, vol. 25, no. 1, pp. 1–18, 2018.
- [6] B. A. Eick, M. D. Smith, and T. B. Fillmore, “Feasibility of Discontinuous Quoin Blocks for USACE Miter Gates,” 2019.
- [7] H. Mahmoud, A. Chulawat, and G. Riveros, “Fatigue and fracture life-cycle cost assessment of a Miter gate with multiple cracks,” *Eng. Fail. Anal.*, vol. 83, no. September 2017, pp. 57–74, Jan. 2018.
- [8] B. A. Eick, B. F. Treece, Zachary R., Spencer Jr., M. D. Smith, S. C. Sweeney, Q. G. Alexander, and S. D. Foltz, “Miter Gate Gap Detection Using Principal Component Analysis,” 2017.
- [9] M. Parno, D. O’Connor, and M. Smith, “High dimensional inference for the structural health monitoring of lock gates,” pp. 1–29, Dec. 2018.
- [10] U.S. Army Corps of Engineers Headquarters, “SMART GATE.” [Online]. Available: <https://www.erdc.usace.army.mil/Media/Fact-Sheets/Fact-Sheet-Article-View/Article/476668/smart-gate/>. [Accessed: 01-Aug-2018].
- [11] Y. Yang, R. Madarshahian, and M. D. Todd, “Bayesian Damage Identification Using Strain Data from Lock Gates,” Springer, 2020, pp. 47–54.
- [12] A. Lee, C. Yau, M. B. Giles, A. Doucet, and C. C. Holmes, “On the Utility of Graphics Cards to Perform Massively Parallel Simulation of Advanced Monte Carlo Methods,” *J. Comput. Graph. Stat.*, vol. 19, no. 4, pp. 769–789, Jan. 2010.
- [13] M. Vega, R. Madarshahian, and M. D. Todd, “A Neural Network Surrogate Model for Structural Health Monitoring of Miter Gates in Navigation Locks,” in *37th International Modal Analysis Conference*, Orlando, Florida, 2020, pp. 93–98.
- [14] J. Brynjarsdóttir and A. O’Hagan, “Learning about physical parameters: the importance of model discrepancy,” *Inverse Probl.*, vol. 30, no. 11, p. 114007, Nov. 2014.
- [15] M. C. Kennedy and A. O’Hagan, “Bayesian calibration of computer models,” *J. R. Stat. Soc. Ser. B (Statistical Methodol.)*, vol. 63, no. 3, pp. 425–464, Aug. 2001.
- [16] Y. Ling, J. Mullins, and S. Mahadevan, “Calibration of multi-physics computational models using Bayesian networks,” *arXiv Prepr. arXiv:1206.5015*, pp. 1–38, Jun. 2012.
- [17] Y. Ling, J. Mullins, and S. Mahadevan, “Selection of model discrepancy priors in Bayesian calibration,” *J. Comput. Phys.*, vol. 276, pp. 665–680, Nov. 2014.